Journal of Magnetic Resonance 212 (2011) 55–63

Contents lists available at ScienceDirect

Journal of Magnetic Resonance

journal homepage: www.elsevier.com/locate/jmr

Tissue specific resonance frequencies of water and metabolites within the human brain

Grzegorz L. Chadzynski [a,*], Benjamin Bender [a], Adriane Groeger [b], Michael Erb [a], Uwe Klose [a]

[a] MR Research Group, Department of Diagnostic and Interventional Neuroradiology, University Hospital Tuebingen, Hoppe-Seyler strasse 3, 72076 Tuebingen, Germany
[b] Department of Neurodegeneration, Hertie Institute for Clinical Brain Research and German Center for Neurodegenerative Disease (DZNE), University of Tuebingen, Hoppe-Seyler Str. 3, 72076 Tuebingen, Germany

ARTICLE INFO

Article history:
Received 8 February 2011
Revised 10 June 2011
Available online 12 July 2011

Keywords:
CSI
Resonance frequency differences
Susceptibility
Proton exchange
Chemical shift displacement

ABSTRACT

Chemical shift imaging (CSI) without water suppression was used to examine tissue-specific resonance frequencies of water and metabolites within the human brain. The aim was to verify if there are any regional differences in those frequencies and to determine the influence of chemical shift displacement in slice-selection direction.

Unsuppressed spectra were acquired at 3 T from nine subjects. Resonance frequencies of water and after water signal removal of total choline, total creatine and NAA were estimated. Furthermore, frequency distances between the water and those resonances were calculated. Results were corrected for chemical shift displacement.

Frequency distances between water and metabolites were consistent and greater for GM than for WM. The highest value of WM to GM difference (14 ppb) was observed for water to NAA frequency distance.

This study demonstrates that there are tissue-specific differences between frequency distances of water and metabolites. Moreover, the influence of chemical shift displacement in slice-selection direction is showed to be negligible.

1. Introduction

In proton magnetic resonance spectroscopy (^{1}H MRS) water signal strongly dominates over metabolite resonances, therefore it is usually suppressed. This approach is straightforward, however it has some disadvantages: signals that are close to the water signal resonance frequency are partially suppressed [1], magnetization transfer effects can hamper the metabolite quantification [2] and water suppressing pulses may introduce phase distortions [3]. MRS without water suppression avoids these problems and additionally allows using unsuppressed water signal for absolute quantification as an internal reference. The potential drawback of this technique is the presence of unwanted sideband artifacts [4]. However, recently a couple of solutions for this problem have been demonstrated [1,3,5,6]. Furthermore, analysis of resonance frequency of the water signal may provide additional information. Current studies have revealed that the resonance frequency of water can be influenced by various factors, like temperature [7–11], pH value [12], water-macromolecule proton exchange [13] and susceptibility [13–16].

The influence of temperature on the contrast of T_1 weighted MR images was proven almost 30 years ago [17]. Furthermore, it was also demonstrated that temperature and pH value affect the resonance frequency of water and other substances [7,12]. This effect can be identified with proton spectroscopy and used for non-invasive temperature and pH mapping. Both physiological parameters can be estimated by calculating the frequency distance between water and metabolites (choline, creatine and N-acetyl aspartate (NAA)) [8,10].

Proton exchange between water and macromolecules and susceptibility effects are known to be responsible for frequency shifts of the water signal. Both effects are suggested to contribute to the contrast between gray (GM) and white matter (WM) within the human brain seen in gradient-echo phase MR images [14–16,18]. Proton exchange effect consists of movement of protons between water and macromolecules, mostly proteins, in exchange between bounded and free water and in spin–spin interactions between free water and macromolecules, as known from magnetization transfer studies [14]. Those mechanisms influence the shielding constant of protons in the water molecule and therefore lead to the shift of the water resonance frequency. They also influence the T_1 and T_2 relaxation times of water and contribute to the phase contrast between

* Corresponding author. Address: Department of Neuroradiology, University Hospital Tuebingen, Hoppe-Seyler strasse 3, D-72076 Tuebingen, Germany. Fax: +49 07071 29 43 71.
E-mail address: grzegorz.chadzynski@med.uni-tuebingen.de (G.L. Chadzynski).

1090-7807/$ - see front matter © 2011 Elsevier Inc. All rights reserved.
doi:10.1016/j.jmr.2011.06.009

GM and WM [14,15]. Another factor responsible for those frequency shifts are susceptibility variations caused by chemical composition and geometrical arrangement of the brain tissue. Non-heme iron compounds [19–22], deoxyhemoglobin and proteins [23,24] were proposed as chemically based sources of those variations. Moreover, the relationship between MR signal phase/frequency and magnetic susceptibility depends on tissue architecture on subcellular and cellular levels that is determined by the structural arrangement of susceptibility inclusions (non-heme iron, deoxyhemoglobin or proteins) [15]. This can be addressed as a geometrically based source of susceptibility variations and it has been found to give a frequency difference between GM and WM of approximately 15.7 parts per billion (ppb) [15]. Recently, Luo et al. [13] have evaluated the contribution of susceptibility variations and proton exchange effects to the shift of the resonance frequency of water. These authors demonstrated that the effects related to susceptibility are approximately two times stronger than proton exchange effects and shift the resonance frequency in the opposite direction.

All these observations refer to the behavior of the water signal only. MRS without water suppression allows accessing the resonance frequency of water and the resonance frequencies of the main metabolites. In combination with chemical shift imaging (CSI) the behavior of resonance frequencies can be described simultaneously for different locations.

In this study, the resonance frequencies of water and metabolites within the central part of the human brain have been examined. A CSI sequence without water suppression at the level of the lateral ventricles was performed to assess the resonance frequencies of water, total choline (tCho), total creatine (tCr) and NAA. The accuracy of data acquisition procedure was corrected with respect to the chemical shift displacement in the slice-selection direction. This has been done by calculating the metabolite-specific chemical shift displacement values. As a result, CSI acquisition was repeated for the slices with the position corrected accordingly.

The aim was to determine if there are any regional differences in resonance frequencies of water and metabolites within the central part of the human brain. Furthermore, the potential influence of chemical shift displacement in slice-selection direction on the mentioned frequency differences was evaluated.

2. Materials and methods

All unsuppressed CSI spectra were acquired with a 3-Tesla MR scanner (TimTrio, Siemens, Erlangen, Germany) equipped with a 32-channel receive-only head coil.

Point resolved spectroscopy (PRESS) localization technique was used for excitation. A 2D CSI matrix was placed above the lateral ventricles, parallel to the line between the anterior and posterior commissures (ac–pc line). Parameters of this acquisition were as follows: TE = 144 ms, TR = 1350 ms, field of view (FOV): $140 \times 140\ mm^2$, excited volume of interest (VOI) $70 \times 70 \times 7\ mm^3$, voxel size: $5.8 \times 5.8 \times 7\ mm^3$, CSI matrix: 24×24 voxels (interpolated to 32×32 voxels), vector size: 512 complex data points, correction for chemical shift-dependent voxel position: −2 ppm (ppm), number of averages: 4, spectral bandwidth: 1000 Hz and weighted phase encoding scheme. With these acquisition parameters total scanning time for the single CSI slice was 15 min 56 s.

Elliptical weighted k-space sampling was used in one of our previous studies [25]. The algorithm omits the high k-space frequencies, while the low k-space frequencies according to the apodization during acquisition were more pronounced to improve the sensitivity over detail and resolution [25]. This scheme reduced the amount of the k-space data to approximately 30% and increased the effective voxel size.

The chemical shift displacement in the slice-selection direction was evaluated to be 1.1 mm, 1.2 mm and 1.9 mm, for total choline, total creatine and NAA slices respectively [26].

Data acquisition was repeated for the slices with the position corrected for chemical shift displacement of evaluated metabolites. Since the difference in position of the slices for tCho and tCr was negligible (approximately 0.1 mm) three CSI slices were acquired: the reference slice, 2nd slice shifted by 1.2 mm and 3rd slice shifted by 1.9 mm in slice-selection direction. Frequency adjustments were done manually and the adjusted volume was expanded from 7 to 11 mm, to cover all three CSI slices. With this manual shimming procedure performed with linear field gradients only, the full width at half maximum of water signal in all measurements was between 13.9 and 17.8 Hz and T_2^* time was from 18 to 23 ms.

For reference measurements, a spherical water phantom (8.07 mmol $NiSO_4$ per 1 dm^3 of distilled water) was used. Water phantom data were collected with the same sequence parameters as volunteer data. Those measurements were done for a single slice only.

In vivo spectra were acquired from nine volunteers, four females and five males, after informed written consent in accordance with the local ethical committee. Ages ranged from 24 to 31 years (mean age 27.5 ± 1.5 years). Volunteers reported no known neurological diseases.

CSI spectra were postprocessed with customized software written under Matlab (2009b, MathWorks, Natick, MA, USA). After the acquisition, data were zero-filled to 2048 complex data points. After the Fourier transformation (FFT), the resonance frequency of the water signal was determined. Subsequently the amplitude of water signal was reduced. This was achieved in time domain by convolution of the unsuppressed FID signal with a Gaussian function (low-pass filter) with full width at half maximum (FWHM) of 5 ms and subtraction of the convoluted line from the original data set [3]. For minimization of the gradient related sidebands, present in the unsuppressed *in vivo* spectra, the FID signal measured for the water phantom was used. Sidebands in *in vivo* voxels were reduced by subtracting the FID signal from the corresponding voxel in water phantom measurements [3]. To reduce noise in postprocessed FID signals, a Hanning filter with time constant of 200 ms was applied. An example of spectra from WM and GM for one representative volunteer is demonstrated in Fig. 1.

Quantitative analysis consisted in comparison of resonance frequencies of water, tCho, tCr and NAA and evaluation of differences in frequency distances between water and those metabolites for voxels in GM and WM. Resonance frequencies and frequency distances were calculated in each CSI slice from three selected regions of interest (ROI) within VOI: central corresponding to GM voxels, left and right, both corresponding to WM voxels. Each single ROI consisted in 6×2 voxels. Both WM ROI were pooled together, so in total there were 12 voxels associated with GM (single ROI) and 24 with WM (both left and right ROI). The influence of chemical shift displacement was evaluated by comparing the frequency distances between water and metabolites calculated for ROI within the reference slice (no correction for chemical shift displacement) with frequency distances calculated between the ROI in reference slice and ROI in 2nd slice (correction for chemical shift displacement between water and tCho and water and tCr) and frequency distance between the ROI in reference slice and ROI in 3rd slice (correction for chemical shift displacement between water and NAA). Since chemical shift displacement occurred in the caudal direction, resonance frequencies of all metabolites were taken from the reference slice, while resonance frequency of water was taken from the 2nd slice (tCho to water and tCr to water frequency

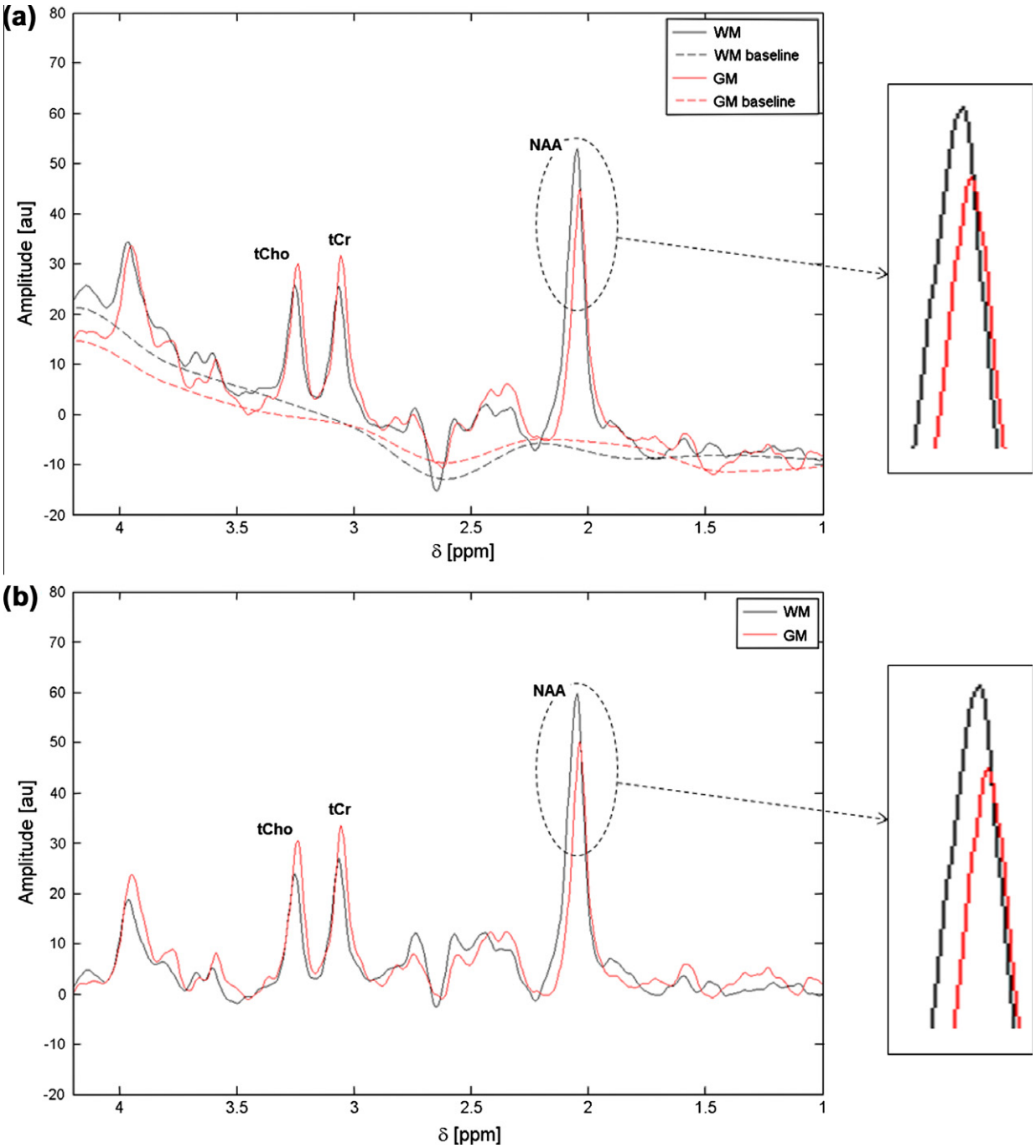

Fig. 1. Typical spectra from single voxel in WM (black) and GM (red) from one representative volunteer before (a) and after (b) baseline correction. The upper part of the NAA peak was magnified for better visualization of the differences in peak position. (For interpretation of the references to color in this figure legend, the reader is referred to the web version of this article.)

distances) and from the 3rd slice (NAA to water frequency distance).

Prior to calculation of frequency distances, all measured resonance frequencies had to be corrected with respect to the systematic intra-slice differences.

Robustness of calculation of resonance frequencies was improved by baseline evaluation for each spectrum. Assessment of baseline was done with shape-preserving piecewise cubic interpolation, which is a part of the Bioinformatics Toolbox (version 3.4) in Matlab. The resonance frequencies of the water and metabolites were estimated by fitting their peaks with a Gauss function. This was done with a least square root differences approach based on the Nedler-Mead simplex algorithm, which is a part of the Curve Fitting Toolbox (version 2.1) in Matlab.

3. Results

Fig. 1 shows a comparison of typical spectra from single voxels in WM and GM before (a) and after (b) baseline estimation. Additional chemical shift correction was applied to all spectra so that the water signal was at the same position (4.7 ppm). It can be noticed that all metabolite peaks (tCho, tCr and NAA) have slightly different positions, while after frequency correction the water

signals in both spectra had the same position. Moreover, the baseline correction has no influence on this effect. The NAA peak in WM is slightly higher compared to the NAA peak in GM. This is in contradiction to the observed NAA concentration [27] but can be explained by T_1 saturation effect, due to the short TR of 1.3 s.

In Fig. 2 the average resonance-frequency maps of tCho, tCr, NAA and water are demonstrated. Frequency maps for the metabolites were calculated from the reference slice, while the frequency maps for water from the 2nd and 3rd slices originate from the same localization as the maps for metabolites. Both frequency maps for water are almost identical: areas with higher frequencies are located in both lateral parts (left and right) and in the medial-anterior part of the VOI, while the medial-posterior part is associated with lower frequency values. In maps for metabolites higher values of frequency in the medial-anterior part is smaller and for the medial-posterior part with lower frequencies it is bigger. Even maps for metabolites demonstrate different pattern. In maps for tCho and tCr the region of higher resonance frequencies associated

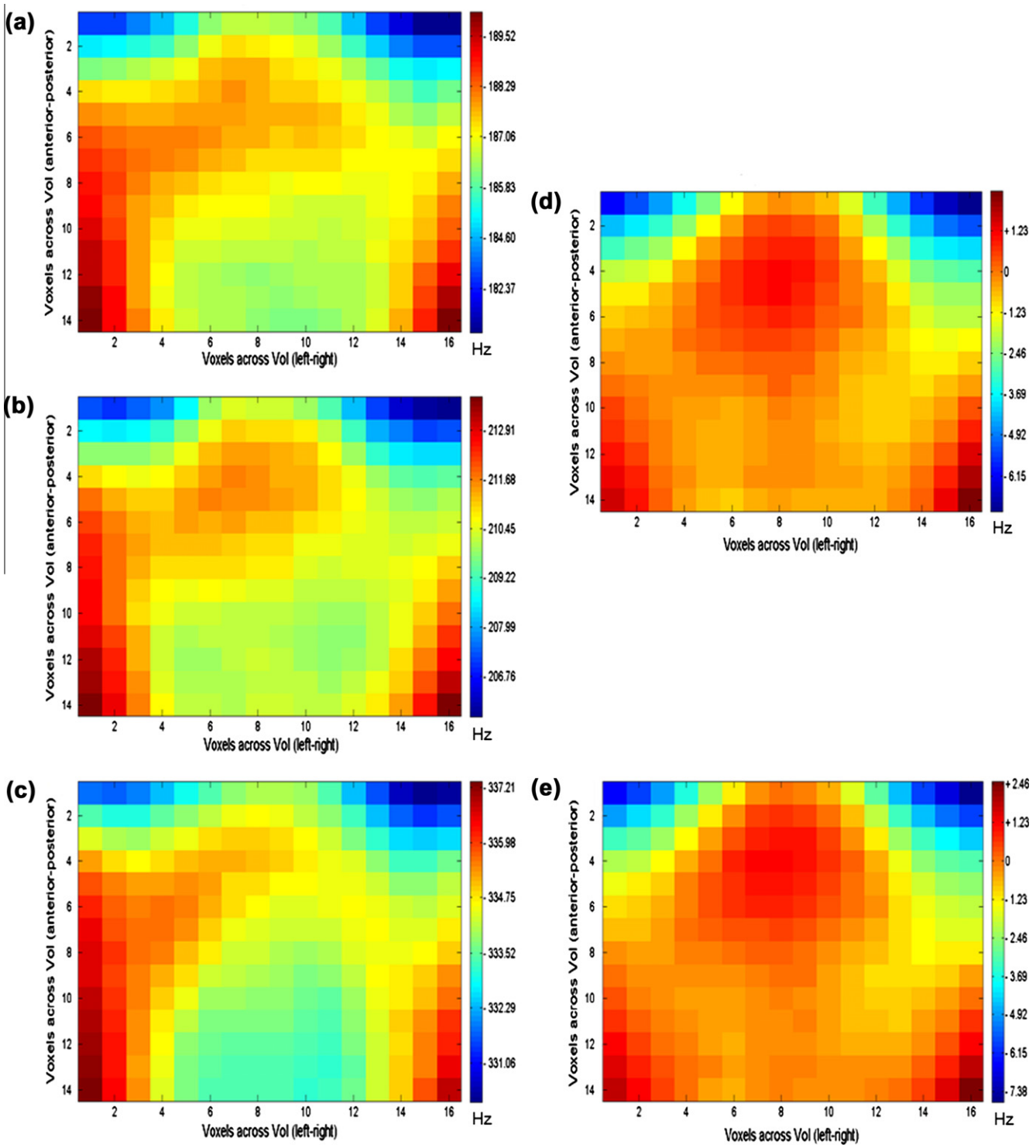

Fig. 2. Resonance frequency maps for tCho (a), tCr (b), NAA (c) and water (d and e). All maps were calculated as an average across all measured volunteers. Frequency maps for metabolites (a–c) were calculated from the reference slice while maps for water from 2nd (d) and 3rd (e) slices, so that they all originate from the same location.

with the medial-anterior part of the VOI is more extensive than for the frequency map for NAA.

Previous finding is confirmed by the frequency profiles seen in Fig. 3. In case of water, voxels from the medial part of the VOI were associated with higher frequency values, whereas for NAA analogous voxels were associated with lower values. For tCho and tCr the increase of frequency in the center of the VOI is compensated by the B_0 field inhomogeneities. This distribution of NAA resonance frequency may correspond to the B_0 field inhomogeneities and appears to show no regional dependence. In contrast to this, frequency profiles of water, tCho and tCr indicate that beside the influence of B_0 field inhomogeneities there is a regional dependency: higher frequencies appear to correspond to GM voxels (medial part of the VOI), while lower frequencies are associated with voxels corresponding to WM (both left and right lateral parts of the VOI).

To minimize the influence of B_0 variations the frequency distance maps between water and tCho, water and tCr and water and NAA (Fig. 4) were calculated and used for further analysis. In this case, the effect of B_0 field inhomogeneities on the frequency distance is compensated because both water and metabolite resonances are affected equally. Fig. 4 shows localizer images and frequency distance maps for all metabolites calculated without and with correction for chemical shift displacement. Rectangular ROI indicate the voxels from which spectra were included in the quantitative analysis (Fig. 4b). It can be seen that maps of frequency distances between water and all metabolites show similar tendencies: frequency distances in the medial part of the VOI are higher compared to both the lateral sides. The most legible differences however, can be noticed for water to NAA frequency distance. Comparison of uncorrected and corrected frequency maps suggests that the correction of chemical shift displacement in slice-selection direction has a minor influence on the frequency distance maps. Both corrected and uncorrected data sets demonstrate similar distribution of frequency distances. This behavior is reproducible for all the measured volunteers.

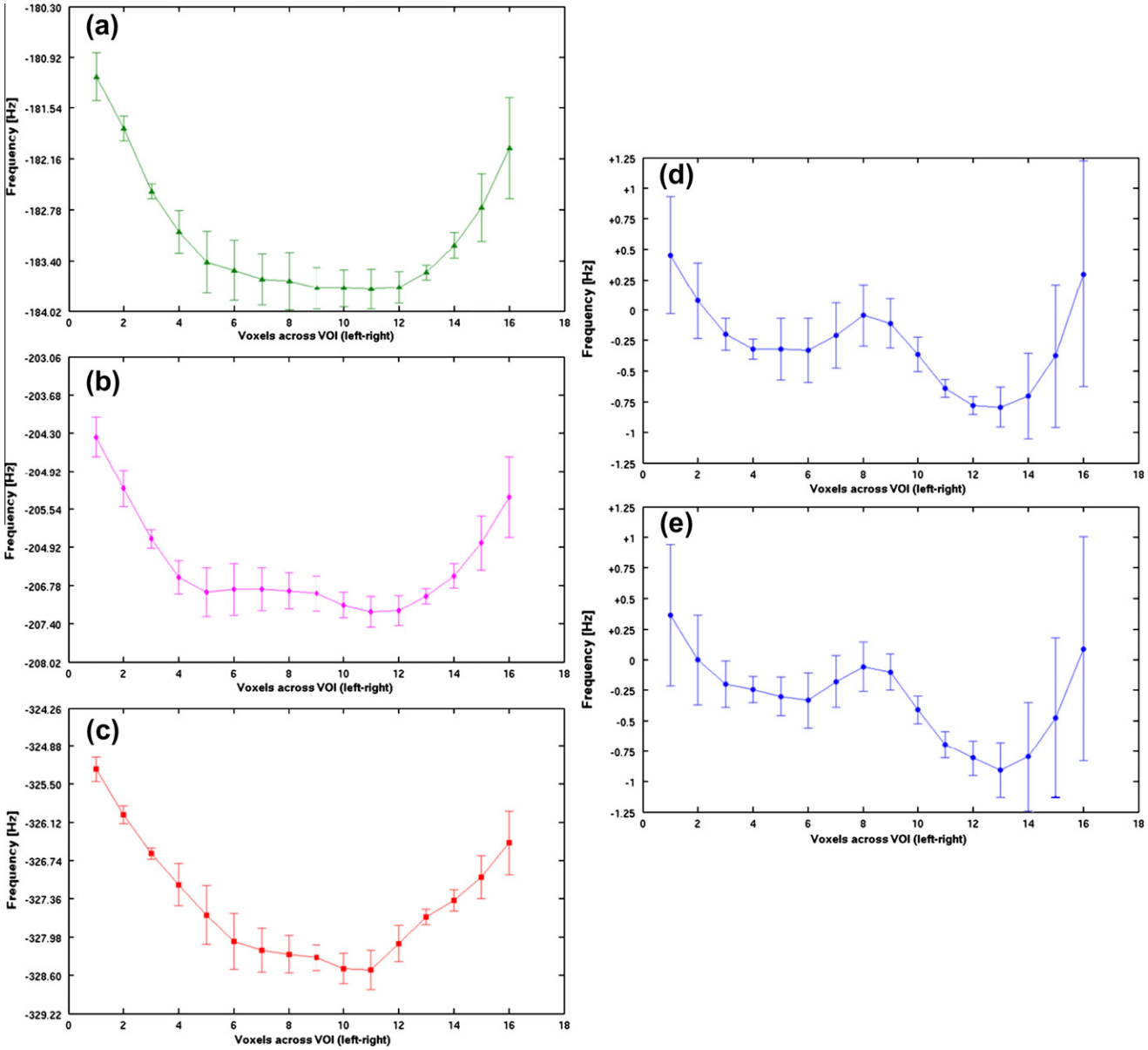

Fig. 3. Resonance frequency profiles for tCho (a), tCr (b), NAA (c) and water (d and e). Profiles were calculated as an average across all measured volunteers, from rows 8th to 12th of the VOI. Frequency profiles for metabolites (a–c) were calculated from the reference slice while profiles for water from the 2nd (d) and 3rd (e) slices, so that they all originate from the same location.

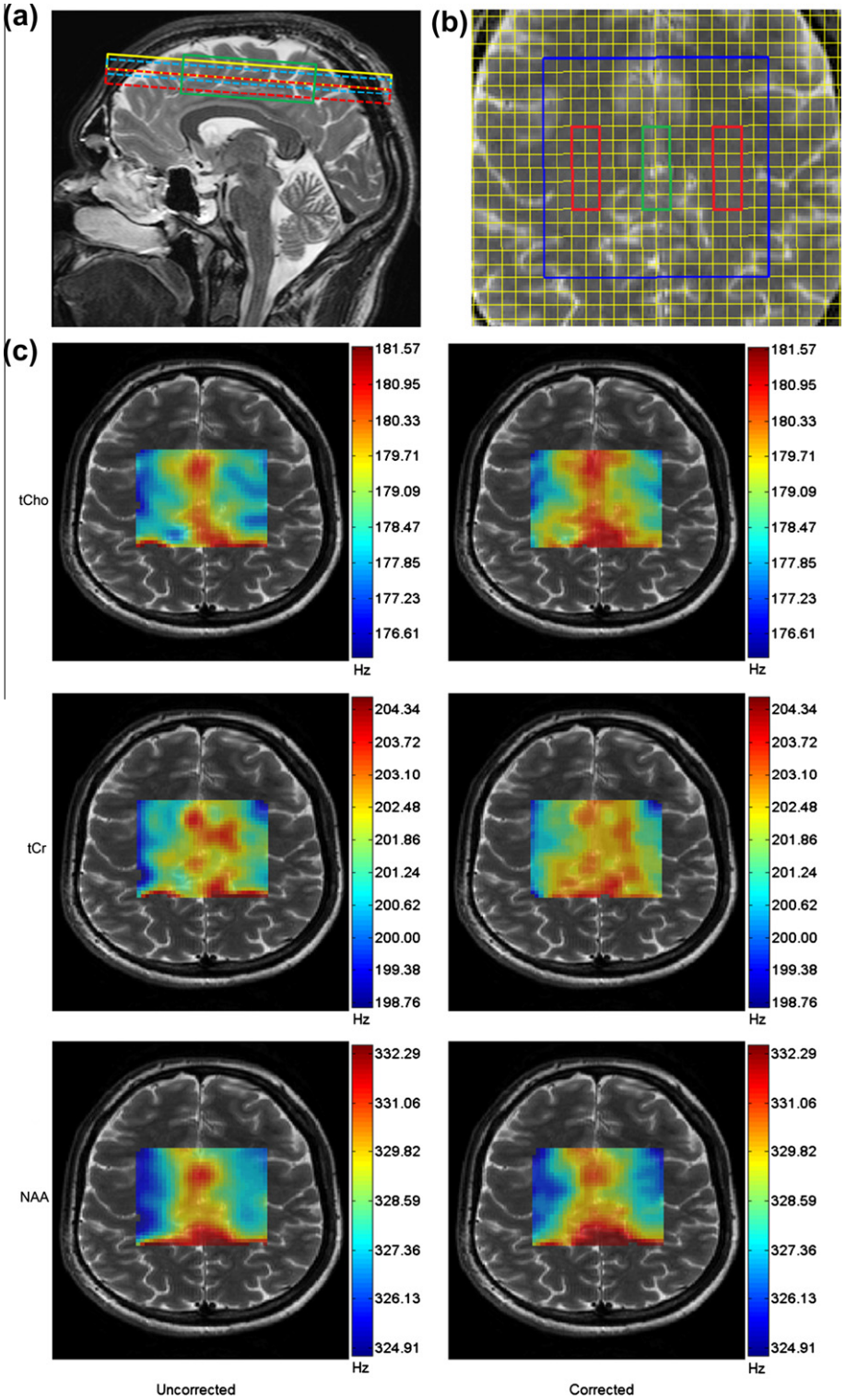

Fig. 4. Sagittal localizer (a), transversal localizer (b) and frequency distance maps between water and all measured metabolites (c) calculated without and with chemical shift displacement correction. Sagittal localizer (a) shows the placement of all measured CSI slices (reference slice: solid yellow, 2nd slice-dashed blue and 3rd slice: dashed red) and the adjusted volume (green). Transversal localizer (b) shows the plane of CSI acquisition, VOI (blue square) and the ROI (red: WM, green: GM), from which voxels were included for quantification. For better visualization of the resonance frequencies distribution, the frequency ranges on each map were adjusted individually. (For interpretation of the references to color in this figure legend, the reader is referred to the web version of this article.)

A comparison of mean values of GM to WM frequency distance differences between water and metabolites calculated without and with correction of chemical shift displacement is illustrated in Fig. 5. The frequency distances between water and tCho, water and tCr and water and NAA in all measured volunteers show similar tendencies. A slight movement of the subject's head between the measurements could be the reason for the observed differences between the corrected and uncorrected data sets. The frequency distances between water and metabolites are greater in GM (blue line) compared to WM (green and red lines). Moreover, the GM

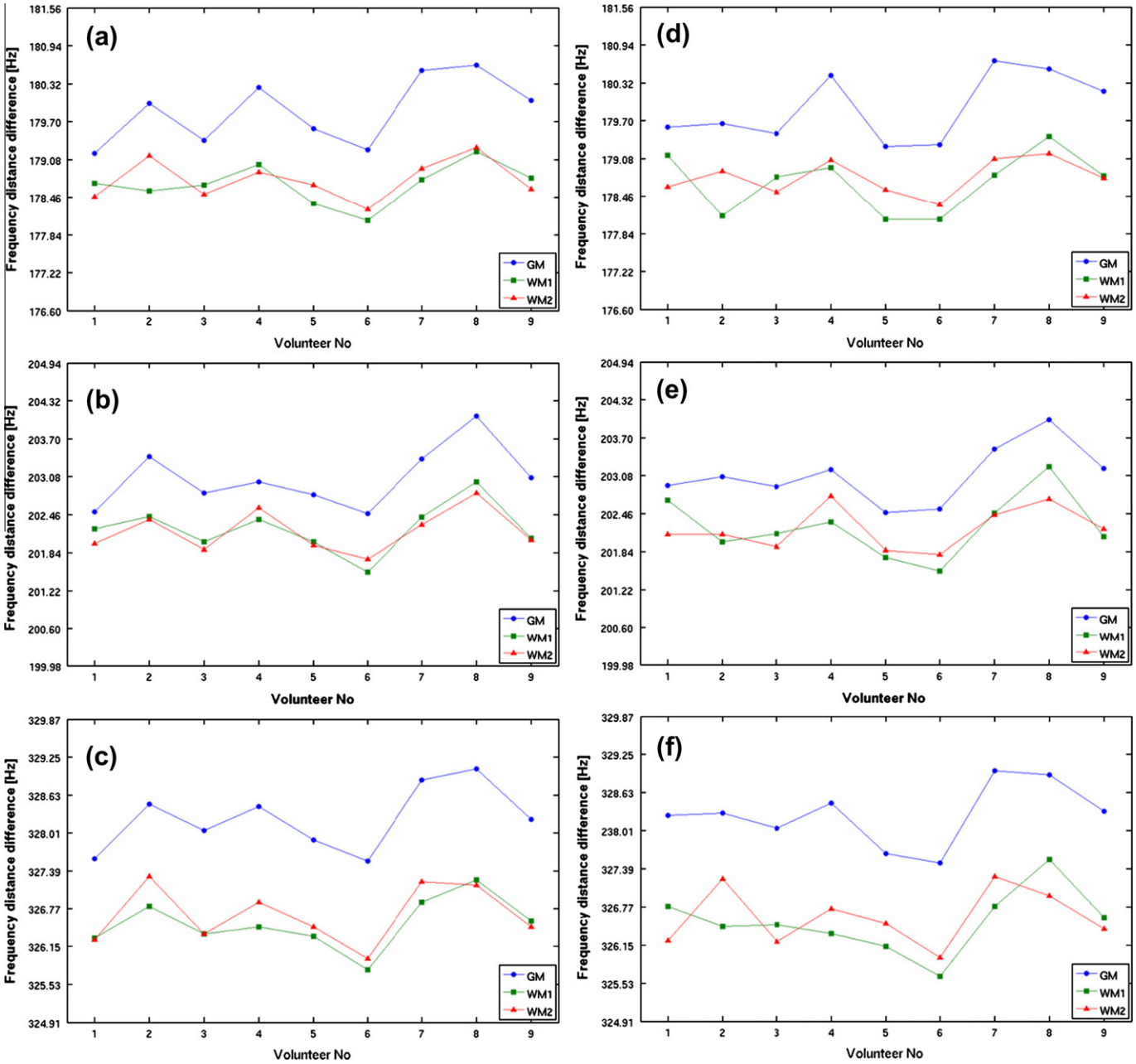

Fig. 5. Mean differences in water to tCho (a and d), water to tCr (b and e) and water to NAA (c and f) frequency distances between WM (red and green) and GM (blue). Values were calculated for all measured volunteers, without (a–c) and with (d–f) correction for chemical shift displacement. (For interpretation of the references to color in this figure legend, the reader is referred to the web version of this article.)

to WM differences in water to tCho and water to tCr frequency distances are smaller compared to the differences obtained for water to NAA frequency distance. One can see that both uncorrected and corrected data sets show a comparable trend, though the applied chemical shift displacement correction appears to increase the intra-volunteer variations in the frequency distances (especially for WM).

Detailed results of the quantitative analysis are presented in Table 1, which contains the mean GM to WM differences in the frequency distances between water and tCho, water and tCr, and water and NAA obtained without and with correction for the chemical shift displacement. In all cases, the frequency distances between water and metabolites were greater for GM than for WM. The highest GM to WM differences were observed for water to NAA frequency distance (13.9 ± 1.9 ppb), while for tCho those differences were approximately 30% less (9.4 ± 2.8 ppb) and for tCr approximately 50% less (7.2 ± 2.1 ppb). A small movement of the subject's head could cause relatively high values of standard deviations that were calculated for single volunteers. The differences between the uncorrected and corrected mean frequency difference values for single volunteers are higher for water to NAA frequency distance (in the range of 3.2 ppb) than for tCho to water and tCr to water frequency distances (both in the range of 1.5 ppb). However, the differences between the mean values calculated across all volunteers are smaller (in the range of 0.4 ppb). Results in Table 1 reveal that the correction for chemical shift displacement leads to an increase of intra-volunteer variations. This is confirmed not only by the plots seen in Fig. 4 but also by higher standard deviations across all volunteers after the correction for chemical shift displacement.

Table 1
Comparison of mean values of differences in water to total choline (tCho), water to total creatine (tCr) and water to NAA frequency distance between GM and WM voxels obtained without and with chemical shift displacement correction.

WM to GM differences	Uncorrected			Corrected		
Volunteer No.	tCho GM–WM [ppb]	tCr GM–WM [ppb]	NAA GM–WM [ppb]	tCho GM–WM [ppb]	tCr GM–WM [ppb]	NAA GM–WM [ppb]
1	5.1 ± 0.9	4.3 ± 1.3	10.7 ± 1.0	4.8 ± 0.2	4.0 ± 1.6	13.9 ± 1.5
2	9.2 ± 0.9	8.0 ± 2.0	11.6 ± 1.7	9.2 ± 1.3	8.1 ± 1.1	11.8 ± 1.3
3	6.4 ± 1.3	6.3 ± 1.2	14.3 ± 0.6	6.7 ± 0.3	6.5 ± 0.7	13.8 ± 1.1
4	9.8 ± 2.0	4.8 ± 1.0	13.1 ± 1.5	10.9 ± 0.4	6.0 ± 1.4	14.6 ± 1.7
5	9.1 ± 0.6	5.9 ± 2.3	12.2 ± 2.4	7.6 ± 1.2	4.4 ± 0.8	10.3 ± 1.4
6	9.4 ± 1.8	7.7 ± 0.8	14.2 ± 0.4	9.4 ± 1.5	7.8 ± 0.5	14.1 ± 1.9
7	13.8 ± 1.3	9.0 ± 1.6	15.5 ± 1.9	14.4 ± 0.9	9.6 ± 1.9	16.7 ± 1.6
8	11.6 ± 0.9	10.1 ± 1.9	15.6 ± 1.6	10.8 ± 1.5	9.2 ± 2.8	14.6 ± 2.1
9	10.4 ± 0.5	9.0 ± 1.9	13.9 ± 0.8	10.7 ± 0.5	9.3 ± 1.7	15.8 ± 2.4
Mean	9.4	7.2	13.5	9.4	7.2	13.9
SD	±2.6	±2.0	±1.7	±2.8	±2.1	±1.9

4. Discussion and conclusions

The aim of this work was to examine whether the known tissue-specific differences in resonance frequency for water also exist for the metabolites: tCho, tCr and NAA. The influence of chemical shift displacement in slice-selection direction on the obtained results was also evaluated. The differences in resonance frequency between WM and GM for water were superimposed by the B_0 field inhomogeneities in CSI measurements, which additionally have a decreased spatial resolution compared to the high-field phase images [15]. Nevertheless, an increase of the water resonance frequency within GM in the central part of the brain could be confirmed (Fig. 2 and 3). A similar effect for tCho, tCr and NAA is not clearly visible in a direct comparison of the GM and WM regions (Fig. 1). Therefore, the frequency differences between water and metabolites within the selected regions were examined.

Calculated frequency distance differences in all cases were higher for voxels associated with GM than for voxels associated with WM. The mean values of the differences between WM and GM calculated across all volunteers (Table 1) were the highest in case of water to NAA frequency distance. Therefore, the pattern seen on water to NAA frequency distance maps (Fig. 4) is the most legible, while the pattern on water to tCho and water to tCr maps appeared to be more dispersed. This behavior could be explained by an analysis of the distribution of resonance frequencies (Fig. 2). The patterns seen on average frequency maps for water and all metabolites were influenced by the B_0 field inhomogeneities. However, the average frequency maps of water (Fig. 2), tCho, tCr and NAA showed different tendencies. Additional effects, which might influence the resonance frequencies, could explain this behavior. This was confirmed by the average frequency profiles (Fig. 3). Both frequency profiles for water frequencies associated with the medial part of the VOI are strongly elevated. Similar behavior can be seen on profiles for tCho and tCr. However, this effect was not as strong for tCho and tCr as it is for water. In contrast, frequency profile for NAA shows no increase of resonance frequencies for voxels corresponding to the medial part of the VOI. These differences in behavior of resonance frequencies of water and metabolites explains why GM to WM differences in frequency distances for water to tCho and water to tCr are approximately 30% (tCho) and 50% (tCr) lower than for water to NAA.

The resonance frequencies of the evaluated metabolites may be influenced by superimposed signals, like myo-inositol (mI), and Glutamine/Glutamate (Glx). However, at the long TE (144 ms) the amplitude of those additional signals (mI and Glx) is reduced compared to what can be seen at the short TE (30 ms) [28,29], thus their influence on the main signals (tCho, tCr and NAA) can be neglected. The same is valid for taurine (Tau) [29].

Reduced k-space sampling enlarged the effective voxel size; however, it was necessary for the reduction of the data acquisition time. Larger effective voxel size increases the signal overlap between adjacent voxels [25] and increases the contribution of the signal from tissue water and cerebro-spinal fluid (CSF), especially in the GM spectra. Nevertheless, frequency differences between WM and GM were still observable for all the measured volunteers. In addition, large dimensions of WM and GM ROI ($11.6 \times 34.8 \times 7\ mm^3$ each) compared to the nominal voxel size ($5.8 \times 5.8 \times 7\ mm^3$) could reduce the influence of this effect.

Correction of chemical shift displacement in slice-selection direction had a minor influence on the obtained GM to WM differences in frequency distances. Chemical shift displacement correction only slightly improved the quality of the frequency distance maps (Fig. 4), but it increased the intra-volunteer variations in the differences in frequency distances between the water and metabolites (Fig. 5, Table 1) as well as the intra-slice variations in the resonance frequency of water. This can be caused by insufficient correction of the intra-slice differences in the resonance frequency of water. However, without this frequency correction, the intra-volunteer differences in frequency distances would be even higher. On the other hand the difference in the localization of the slices caused by the chemical shift displacement is from 1.3 mm (tCho, tCr) to 1.9 mm (NAA), therefore the influence of this effect on the obtained results could be neglected.

It was previously shown that resonance frequency may be influenced by temperature [7–11,17,18], pH value [12], proton exchange [16] and susceptibility [13,15,19] The differences in water to NAA resonance frequency distances between WM and GM would correspond to a temperature difference of approximately 1 K [8]. The temperature sensitivity for the evaluated metabolites differ maximally by 5% [8]. Therefore, temperature differences are not a likely explanation. Relatively low sensitivity of the endogenous substances to pH changes [12] causes the influence of the pH on tCho, tCr and NAA to be negligible. Theoretically, resonance frequency of water could be affected by the pH changes. However, then the differences in the frequency distances between WM and GM should be the same for all metabolites. This is not the case since the greatest differences between WM and GM is observed for the water to NAA frequency distance (Table 1). On the other hand, comparable differences in the resonance frequency of water between WM and GM have been shown by phase image studies [13,15,19]. He et al. [15] reported an approximate difference of 15.7 ppb. This is very close to the highest difference found in this study (13.9 ppb, Table 1), which suggest that the resonance frequency of water is shifted while the resonance frequency of NAA appears to be constant. This is in good agreement with Fig. 2. The slight difference to the results by He et al. [15] can be

explained by the larger voxel size and therefore, higher contribution of partial volume effects.

For that reason, the most probable explanation of the observed GM to WM frequency distance differences are the influences of proton exchange and susceptibility effects also found in the phase images. In addition to phase imaging studies it has been found that not only the resonance frequency of water is influenced but also the resonance frequencies of tCho and tCr. This could explain the smaller differences in values between GM and WM obtained for tCho to water and tCr to water compared to NAA to water frequency distances (Table 1). It is known that water is present in both extracellular and intracellular spaces, while NAA is characteristic to intraneuronal space [30]. Therefore, different behavior of the three metabolites could be caused by microstructural arrangement of the brain tissue and its alignment to the B_0 field, which according to He et al. [15] may enhance the susceptibility effects. Additionally, in this study, the central part of the brain was examined. In this region, the WM fibers are mostly parallel to the B_0 field (corticospinal tract). In other localizations within the WM, where fibers have different alignment, one could expect different results. Nevertheless, measurements that are more detailed would be necessary to clarify to what extent those effects contribute to the shifts in the resonance frequencies of water and metabolites.

In conclusion, we demonstrated that in the central part of the brain there are regional differences in frequency distances between the water and metabolites. We also found that chemical shift displacement has a minor influence on the obtained results and therefore, correction of this effect can be neglected. This suggests that the water signal measured with CSI without water suppression may contain relevant information and this can be used not only as an internal reference in absolute quantification. The analysis of unsuppressed spectra can also provide important additional information about tissue-dependent variations of resonance frequencies of water and metabolites.

Acknowledgments

The authors would like to acknowledge Dr. Filip Jiru from MR-Unit at Department of Radiodiagnostic and Interventional Radiology in Institute for Clinical and Experimental Medicine in Prague, Czech Republic for helping with software development.

The German Research Foundation (DFG KL 1073/7-1) financially supported this study.

References

[1] Z. Dong, W. Dreher, D. Leibfritz, Experimental method to eliminate frequency modulation sidebands in localized in vivo ^{1}H MR spectroscopy acquired without water suppression, Magn. Reson. Med. 51 (2004) 602–606.
[2] D. Leibfritz, W. Dreher, Magnetization transfer MRS, NMR Biomed. 14 (2001) 65–76.
[3] G.L. Chadzynski, U. Klose, Chemical shift imaging without water suppression at 3T, Magn. Reson. Imaging 28 (2010) 669–675.
[4] D.B. Clayton, M.A. Eliott, J.S. Leigh, R.E. Lenkinski, ^{1}H spectroscopy without solvent suppression: characterization of signal modulations at short echo times, J. Magn. Reson. 153 (2001) 203–209.
[5] R.E. Hurd, D. Gurr, N. Sailasuta, Proton spectroscopy without water suppression: the oversampled J-resolved experiment, Magn. Reson. Med. 40 (1998) 343–347.
[6] T.W. Nixon, S. McIntyre, D.L. Rothman, R.A. de Graf, Compensation of gradient-induced magnetic field perturbations, J. Magn. Reson. 192 (2008) 209–217.
[7] K. Kuroda, Y. Suzuki, Y. Ishihara, K. Okamoto, Y. Suzuki, Temperature mapping using water proton chemical shift obtained with 3D-MRSI: feasibility in vivo, Magn. Reson. Med. 35 (1996) 20–29.
[8] M. Zhu, A. Bashir, J.J. Ackerman, D.A. Yablonskiy, Improved calibration technique for in vivo proton MRS thermometry for brain temperature measurement, Magn. Reson. Med. 60 (2008) 536–541.
[9] R.S. Samson, J.S. Thornton, M.A. McLean, S.C.R. Williams, P.S. Tofts, ^{1}H-MRS internal thermometry in test-objects (phantoms) to within 0.1 K for quality assurance in long-term quantitative MR studies, NMR Biomed. 19 (2006) 560–565.
[10] R. Corbett, A. Laptook, P. Weatherhall, Noninvasive measurements of human brain temperature using volume-localized proton magnetic resonance spectroscopy, J. Cerebr. Blood Flow Metab. 17 (1997) 363–369.
[11] A.R. Laptook, R.J.T. Corbett, R. Sterett, D. Garcia, G. Tollefsbol, Quantitative relationship between brain temperature and energy utilization rate measured in vivo using ^{31}P and ^{1}H magnetic resonance spectroscopy, Pediatr. Res. 38 (1995) 919–925.
[12] D. Coman, H.K. Trubel, R.E. Rycyna, F. Hyder, Brain temperature and pH measured by ^{1}H chemical shift imaging of thulium agent, NMR Biomed. 22 (2009) 229–239.
[13] J. Luo, X. He, D.A. d'Avignon, J.J.H. Ackerman, D.A. Yablonskiy, Protein-induced water ^{1}H MR frequency shifts: contributions from magnetic susceptibility and exchange effects, J. Magn. Reson. 202 (2010) 102–108.
[14] R.M. Henkelman, G.J. Stanisz, S.J. Graham, Magnetization transfer in MRI: a review, NMR Biomed. 14 (2001) 57–64.
[15] X. He, D.A. Yablonskiy, Biophysical mechanisms of phase contrast in gradient echo MRI, Proc. Natl. Acad. Sci. 106 (2009) 13558–13563.
[16] K. Zhong, J. Leupold, D. von Elverfeldt, O. Speck, The molecular basis for gray and white matter contrast in phase imaging, NeuroImage. 40 (2008) 1561–1566.
[17] D.L. Parker, V. Smith, P. Sheldon, L.E. Crooks, L. Fussel, Temperature distribution measurements in two-dimensional MRI imaging, Med. Phys. 10 (1983) 321–325.
[18] C. Childs, Y. Hiltunen, R. Vidyasagar, R.A. Kauppinen, Determination of regional brain temperature using proton magnetic resonance spectroscopy to assess brain–body temperature differences in healthy human subjects, Magn. Reson. Med. 57 (2007) 59–66.
[19] J.H. Dyun, P. van Gelderen, T.Q. Li, J.A. de Zwart, A.P. Koretsky, M. Fukunaga, High-field MRI of brain cortical substructure based on signal phase, Proc. Natl. Acad. Sci. 104 (2007) 11796–11801.
[20] M.A. Haacke, N.Y.C. Cheng, M.J. HouseJ, Q. Liu, J. Neelavalli, R.J. Ogg, A. Khan, M. Ayaz, W. Kirsch, A. Obenaus, Imaging iron stores in the brain using magnetic resonance imaging, Magn. Reson. Imaging 23 (2005) 1–25.
[21] J.F. Schenck, E.A. Zimmerman, High-field magnetic resonance imaging of brain iron: a birth of a biomarker?, NMR Biomed 17 (2004) 433–445.
[22] J.F. Schenck, Magnetic resonance imaging of brain iron, J. Neurol. Sci. 207 (2003) 99–102.
[23] W.M. Spees, D.A. Yablonskiy, M.C. Oswood, J.J.H. Ackerman, Water proton MR properties of human blood at 1.5 Tesla: magnetic susceptibility, T_1, T_2, T_2^* and non-Lorenzian signal behavior, Magn. Reson. Med. 45 (2001) 533–542.
[24] X. He, M. Zhu, D.A. Yablonskiy, Validation of oxygen extraction fraction measurement by qBOLD technique, Magn. Reson. Med. 60 (2008) 882–888.
[25] A. Groeger, G. Chadzynski, J. Godau, D. Berg, U. Klose, Three-dimensional magnetic resonance spectroscopic imaging in the substantia nigra of healthy controls and patients with Parkinson's disease, Eur Radiol., [Epub ahead of print].
[26] M.A. Bernstein, K.F. King, X.J. Zhou, Imaging gradients, in: M.A. Bernstein (Ed.), Handbook of MRI Pulse Sequences, Elsevier Inc., Burlington, MA, 2004, pp. 243–273.
[27] Y. Wang, S.J. Li, Differentiation of metabolic concentrations between gray matter and white matter of human brain by in vivo ^{1}H magnetic resonance spectroscopy, Magn. Reson. Med. 39 (1998) 28–33.
[28] F. Traeber, W. Block, R. Lamerichs, J. Gieseke, H.H. Schild, 1H metabolite relaxation times at 3.0 Tesla: measurements of T_1 and T_2 values in normal brain and determination of regional differences in transverse relaxation, J. Magn. Reson. Imaging 19 (2004) 537–545.
[29] L. Xin, G. Gambarota, V. Mlynarik, R. Gruetter, Proton T_2 relaxation time of J-coupled cerebral metabolites in rat brain at 9.4 T, NMR Biomed. 21 (2008) 396–401.
[30] J.R. Moffet, B. Ross, P. Arun, C.N. Madhavarao, A.M.A. Namboodiri, N-Acetylaspartate in the CNS: from neurodiagnostics to neurobiology, Prog. Neurobiol. 81 (2007) 89–131.